



New piperazine and morpholine derivatives: Mass spectrometry characterization and evaluation of their antimicrobial activity

Maria Assunta Acquavia^a, Maria Grazia Bonomo^{a,c,*}, Giuliana Bianco^a, Giovanni Salzano^{a,c}, Carmine Gaeta^b, Patrizia Iannece^b, Angela Di Capua^{a,*}, Federica Giuzio^{a,c}, Carmela Saturnino^a

^a Università degli Studi della Basilicata, Dipartimento di Scienze, Viale dell'Ateneo Lucano 10, Potenza, Italy

^b Università degli Studi di Salerno, Dipartimento di Chimica e Biologia, Via Giovanni Paolo II 132, Fisciano, Italy

^c Spinoff TNcKILLERS, Viale Dell'Ateneo Lucano 10, Potenza 85100, Italy

ARTICLE INFO

Keywords:

Piperazine/morpholine derivatives
HRMS
MSⁿ
Structural characterization
Antimicrobial activity

ABSTRACT

Recently, pharmaceutical research has been focused on the design of new antibacterial drugs with higher selectivity towards several strains. Major issues concern the possibility to obtain compounds with fewer side effects, at the same time effectively overcoming the problem of antimicrobial resistance. Several solutions include the synthesis of new pharmacophores starting from piperazine or morpholine core units. Mass spectrometry-based techniques offer important support for the structural characterization of newly synthesized compounds to design safer and more effective drugs for various medical conditions. Here, two new piperazine derivatives and four new morpholine derivatives were synthesized and structurally characterized through a combined approach of Fourier transform-ion cyclotron resonance (FT-ICR) and Linear Trap Quadrupole (LTQ) mass spectrometry. The support of both high-resolution and low-resolution mass spectrometric data namely accurate mass measurements, isotopic distribution and MSⁿ spectra, was crucial to confirm the success of the synthesis. These compounds were further evaluated for inhibitory activity against a total of twenty-nine Gram-positive and Gram-negative bacteria to determine the action spectrum and the antimicrobial effectiveness. Results demonstrated compounds' antimicrobial activity against many tested bacterial species, providing an inhibitory effect linked to different chemical structure and suggesting that the new-synthesized derivatives could be considered as promising antimicrobial agents.

1. Introduction

Since the introduction of the first antibiotics, in the early 1900 s, the modern medicine has greatly changed, positively affecting and extending the average human lifespan. The period between 1950 and 1960 has been a golden age for antibiotics discovery and, till to year 2000, antibiotics' production has significantly increased [1], due to their use for the treatment of several pathologies other than infectious diseases, such as cancer treatment, organ transplants and open-heart surgery [2]. Besides human use, antibacterial drugs have also been adopted for nontherapeutic applications, such as growth promoters for animals to improve feed efficiency [3]. Their extending use for both human and animal purposes has resulted in the rapid rise of antimicrobial resistance (AMR), leading to the impossibility to effectively treat numerous infections [4]. AMR is defined as the presence of a genetically acquired or mutated resistance mechanism, categorizing the pathogen as resistant or

susceptible based on the application of a set cut-off in a phenotypic laboratory test [5]. To date, antimicrobial resistance is a significant global health concern, as it could cause prolonged illnesses as well as higher mortality rates and increased healthcare costs. Due to these challenges, multifaced national and international strategies are recommended to improve infection prevention and control practices, thus reducing the antibiotics request and improving the production of new ones. The development of new active molecules raises the question related to the need to identify target compounds either with new modes of action or with new target interactions and established mechanism of action [6]. Among the several solutions available, one of the options is the synthesis of new pharmacophores starting from piperazine or morpholine core units.

Piperazine ranks as the third most common N-heterocycle appearing in small pharmaceutical molecules and it still continues to be a privileged structural motif in drug discovery [7]. It consists of a

* Corresponding authors at: Università degli Studi della Basilicata, Dipartimento di Scienze, Viale dell'Ateneo Lucano 10, Potenza, Italy.

E-mail addresses: mariagrazia.bonomo@unibas.it (M.G. Bonomo), angela.dicapua@unibas.it (A. Di Capua).

<https://doi.org/10.1016/j.jpba.2024.116202>

Received 30 January 2024; Received in revised form 26 April 2024; Accepted 3 May 2024

Available online 12 May 2024

0731-7085/© 2024 The Authors. Published by Elsevier B.V. This is an open access article under the CC BY license (<http://creativecommons.org/licenses/by/4.0/>).

six-membered ring with two nitrogen atoms at positions 1 and 4 in the ring. Piperazine is a freely water and ethylene glycol soluble compound and the presence of two nitrogen atoms confers weak basic properties (pK_b of 5.3 and 9.7 at 25°C) [8]. Most of the drugs containing piperazine scaffold are substituted either on both or on a single nitrogen atom. Moreover, piperazine often serves as a connecting moiety, linking two segments of a drug, or as an additional component to fine-tune the physicochemical characteristics of the drug. In general, its high polar surface area and relative structural rigidity allow to improve absorption, distribution, metabolism, and excretion properties [9]. As regard to morpholine, it is structurally related to piperazine by the substitution of one N atom with oxygen in the six-membered ring. Although morpholine is a relatively strong base (pK_b of 5.3), ring substitution could increase compound basicity as pK_a could vary between 8.0 and 6.1 [10]. While the lipophilicity of molecules containing morpholine scaffold primarily relies on their specific substitutions, the ring itself exhibits well-balanced lipophilic-hydrophilic properties, demonstrating desirable characteristics for pharmaceutical applications. Both piperazine and morpholine are versatile building blocks that can be easily modified and functionalized to create several chemical structures, with enhanced efficacy, specificity, and pharmacokinetic properties. Their derivatives have been recognized for a wide array of therapeutical effects, encompassing analgesic, anti-inflammatory, antihyperlipidemic properties, as well as exhibiting anticancer and antimicrobial properties [11,12]. Therefore, they can serve as starting point for designing new antibiotics

with improved potency and expanded spectrum of activity against multidrug-resistant pathogens.

Due to the current demand for new antimicrobials able to address life-threatening infections caused by the worldwide dissemination of multidrug-resistant bacterial pathogens, in this work new piperazine and morpholine derivatives (Fig. 1) with potential antibacterial activity have been synthesized, structurally characterized by mass spectrometry, both low and high-resolution MS, and evaluated for their antibacterial activity.

2. Materials and methods

2.1. Synthesis of derivative (1)

For the synthesis of piperazine derivative (1), an equivalent of 2-phenylbutanoyl chloride was dissolved in toluene at 110.6°C under continuous stirring. Then, an equivalent of Na₂CO₃ and 3-(4-methylpiperazin-1-yl) propan-1-amine were added. The reaction mixture was left for 3 hours under continuous stirring. The product was purified by crystallization in acetonitrile.

2.2. Synthesis of derivative (2)

For the synthesis of piperazine derivative (2), an equivalent of 2-cyclohexyl-2-phenylacetyl chloride was dissolved in toluene at

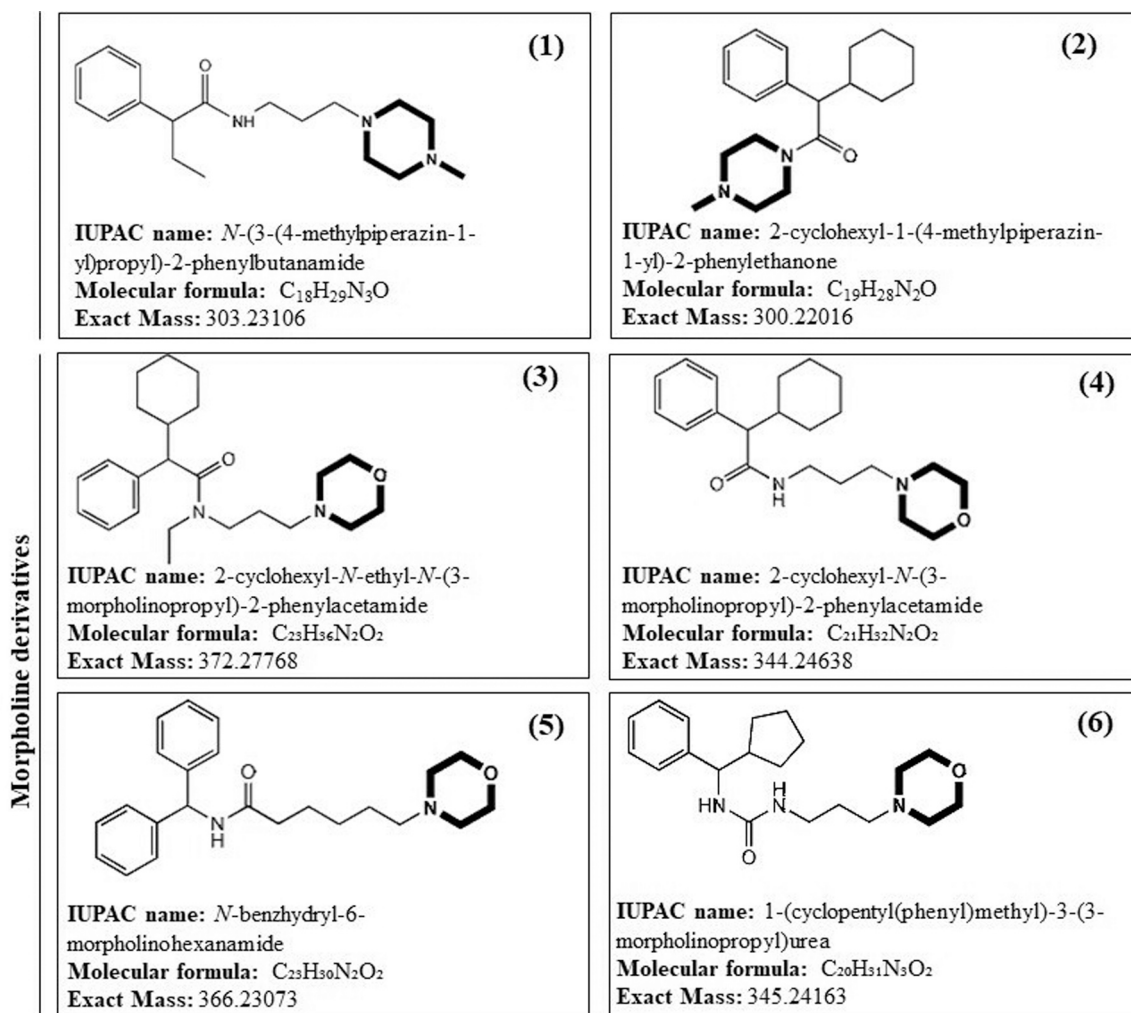


Fig. 1. IUPAC name, structure, molecular formula and exact mass of new synthesized piperazine ((1) and (2)) and morpholine ((3), (4), (5), (6)) derivatives characterized and tested for antimicrobial activity.

110.6°C under continuous stirring. Then, an equivalent of Na₂CO₃ and N-methylpiperazine were added. The reaction mixture was left for 3 hours under continuous stirring. The product was purified by crystallization in acetonitrile.

2.3. Synthesis of derivatives (3), (4), (5) and (6)

For morpholine derivatives, a previous optimized synthesis was used [13]. Briefly, a suitable carboxylic acid was refluxed with SOCl₂ in benzene for 4 h and then evaporated in vacuo to yield the crude acyl chloride which then reacted with N-(3-aminopropyl) morpholine in benzene in presence of Na₂CO₃ for 4–5 h to give morpholine derivatives. (Caution! Exposure to benzene has been linked with a higher risk of cancer, safety precautions are strongly recommended.)

2.4. Mass spectrometric analysis

For each piperazine and morpholine derivative, a stock solution at a concentration of 1 mg/ml in MeOH was prepared. For a complete solubilization of the compounds, all prepared solutions were sonicated for 15 min (T = 25°C) with a Sonorex Super RK 100/H sonicator (Bandelin electronic, Berlin, Germany). Then, stock solutions were diluted to a final concentration of 1 µg/ml, filtered with 0.2 µm PTFE filters (Whatman Puradisc Syringe Filter) and directly injected into the mass spectrometers. High-resolution ESI mass spectra were acquired in positive ion mode with a 7 T solarix XR FT-ICR MS (Bruker Daltonik GmbH, Bremen, Germany). The capillary voltage was set to 3.9 kV, with a nebulizer gas pressure of 1.2 bar and dry gas flow rate of 4 L/min at 200°C. Mass spectra were acquired in a mass range of 100–2000 *m/z* using a time-domain ion signal size of 16 mega-words and an ion accumulation time of 0.1 s. The number of scans was set to 50. Before the analysis, the mass spectrometer was externally calibrated with NaTFA. In order to study the fragmentation pathway of each derivative, MSⁿ experiments were conducted by using a linear trap quadrupole (LTQ) mass spectrometer (Thermo Fisher Scientific, Bremen, Germany). For ESI(+)-MSⁿ spectra acquisition, source voltage was set to 4.5 kV, temperature of the heated capillary was set to 350°C, the capillary voltage was set to + 45 V, and the tube lens' voltage was set to – 75 V. The sheath gas (N₂) flow rate was 5 arbitrary units (a.u). Collision energies were optimized for each precursor ion. Mass spectrometric data were imported, elaborated, and plotted by SigmaPlot 11.0 (Systat Software, London, UK).

2.5. Antimicrobial activity

2.5.1. Bacterial strains and growth conditions

The different derivatives were tested against a panel of bacterial strains shown in Table S1. A total of twenty-nine strains of the culture collection of the Department of Sciences, University of Basilicata, Potenza, Italy, were employed as screening microorganisms for this study. All strains were maintained as freeze-dried stocks in reconstituted (11% w/v) skim milk, containing 0.1% w/v ascorbic acid and routinely cultivated in optimal growth conditions [14] (Table S1). These bacteria were chosen in order to represent the diversity of food-borne (label from 1 to 20) and environment-borne (label from 21 to 29) Gram-positive and Gram-negative species.

2.5.2. Agar well diffusion assay and minimum inhibitory concentration (MIC)

Antimicrobial activity was determined by standard agar well diffusion assay as described by Bonomo et al. [15]. For each strain, a subculture in a specific broth was obtained from the active stock culture by 1% (v/v) inoculum and incubated overnight at the corresponding culture temperature. 200 µL of each subculture was used to inoculate the agar media (to achieve a final concentration of 10⁶ CFU/ml) and distributed into Petri plates. 50 µL of each compound (50 mg/ml) was

poured into wells (6 mm diameter) bored in the agar plates and then the plates were incubated at optimal growth conditions for each strain. Organic solvent was used as negative control while chloramphenicol antibiotic was used as positive control. The experiment was performed in triplicate and the antimicrobial activity of each extract was expressed in terms of zone of inhibition diameter mean (in mm) produced by the respective extract after 24 h of incubation. An inhibition zone <10 mm indicated a low antimicrobial activity; 10 < zone of inhibition <15 mm, a middle antimicrobial activity; a zone of inhibition >15 mm, a high antimicrobial activity.

Then, each compound was screened to determine the minimum inhibitory concentrations (MICs) in order to evaluate the antimicrobial effectiveness of each compound against different bacterial strains by the agar well diffusion method [15]. Each specific medium inoculated with the strain subculture was distributed into Petri plates and different concentrations of compounds, ranging from 1.562 mg/ml to 50 mg/ml, were poured into wells bored in the agar plates and the plates were incubated for 24 h. After incubation, the MIC was calculated as the lowest concentration of the compound inhibiting the growth of bacterial strains. The MIC values were done in triplicate.

3. Results and discussion

In this study, ESI (+)-FT ICR MS spectra acquired for piperazine derivative (1) showed a protonated adduct, [M+H]⁺, at *m/z* 304.23882 (C₁₈H₃₀N₃O⁺, RMS error 1.6 ppm), alongside with two other mass signals corresponding to the two isotopologues, A+1 and A+2 at *m/z* 305.23886 (C₁₇¹³C₁H₃₀N₃O⁺, RMS error 1.7 ppm) and *m/z* 306.23901 (C₁₆¹³C₂H₃₀N₃O⁺, RMS error 2.2 ppm), respectively, due to the presence of ¹³C isotopes. The correctness of this assignment was verified both in terms of mass accuracy and relative intensity of isotopologues signals (Table 1). For derivative (2), the elemental composition was confirmed by its accurate mass, as a protonated adduct was observed at *m/z* 301.22784 (C₁₉H₂₉N₂O⁺; RMS error 1.3 ppm), alongside with signals related to isotopologues A+1 at *m/z* 302.22829 (C₁₈¹³C₁H₂₉N₂O⁺; RMS error 2.8 ppm) and A+2 at *m/z* 303.22847 (C₁₇¹³C₂H₂₉N₂O⁺; RMS error 3.4 ppm) (Table 1).

The fragmentation behaviour of both piperazine compounds was studied by collision induced dissociation (CID) using a linear ion trap mass spectrometer (LTQ-MS), thus facilitating structure elucidation based on MSⁿ scans. For derivative (1), a single signal at *m/z* 204.0 was obtained by fragmenting precursor ion at *m/z* 304.1, which was isolated with a window of 6 *m/z* in order to include the whole isotopologue cluster of the protonated molecule. A collision energy of 7.4 eV was applied for MS/MS studies. Base peak at *m/z* 204.0 ([C₁₃H₁₈NO]⁺) was due to the characteristic neutral loss of N-methylpiperazine (-100 Da, C₅H₁₂N₂) [16]. (1) structure was confirmed by MS³ experiments, by fragmenting ion at *m/z* 204.0 with a collision energy of 9.8 eV. The obtained MS³ spectra is reported in Fig. 2, alongside with the proposed fragmentation scheme. Two major fragments were observed at *m/z* 119.0 (C₉H₁₁⁺) and *m/z* 148.0 (C₁₀H₁₂O⁺), due to the cleavage of the bond with α-carbon and amide bond, respectively.

In order to confirm the structure of the novel piperazine derivative (2), precursor ion at *m/z* 301.1 was isolated and fragmented by CID with a collision energy of 7.4 eV, thus obtaining a base peak at *m/z* 101.0 corresponding to protonated methyl piperazine (C₅H₁₃N₂⁺). A signal at *m/z* 173.0 (C₁₃H₁₇⁺), obtained from the loss of a C₆H₁₂N₂O unit by intramolecular elimination and formation of a new π bond in the detected product ion, was observed. Furthermore, a neutral loss of a C₂H₅N unit through the opening of the cyclic structure of N-methylpiperazine generated a fragment ion at *m/z* 258.0 (C₁₇H₂₄NO⁺). Product ion at *m/z* 101.0 was further fragmented by applying a collision energy of 10.5 eV. Three major fragments were obtained at *m/z* 84.0 (C₅H₁₀N⁺), due to the loss of NH₃ following the opening of the piperazine ring, *m/z* 70.0 (C₄H₈N⁺), due to the loss of a CH₂N unit and *m/z* 58.0 (C₃H₈N⁺) obtained from the loss of a C₂H₅N unit (Figure S1). The

Table 1

Accurate mass values, relative intensity and mass accuracy, expressed as RMS errors in ppm, of the protonated adducts and isotopologues of new synthesized piperazine (1) and (2) derivatives.

Compound Molecular Formula Exact mass	m/z^a	Relative Intensity (%)	Mass accuracy in RMS ^b ppm	ESI-(+)-FT ICR MS spectra
(1) $C_{18}H_{30}N_3O$ 303.23106	$[M+H]^+$ 304.23882	100	1.6	
	$[M+H+1]^+$ 305.23886	19.27	1.7	
	$[M+H+2]^+$ 306.23901	1.69	2.2	
(2) $C_{19}H_{28}N_2O$ 300.22016	$[M+H]^+$ 301.22784	100	1.3	
	$[M+H+1]^+$ 302.22829	20.50	2.8	
	$[M+H+2]^+$ 303.22847	2.00	3.4	

^a Calculated as mean of 5 m/z measurements.

^b Mass accuracy reported as root-mean-square (RMS) in parts per million (ppm) of five ($n=5$) m/z measurements.

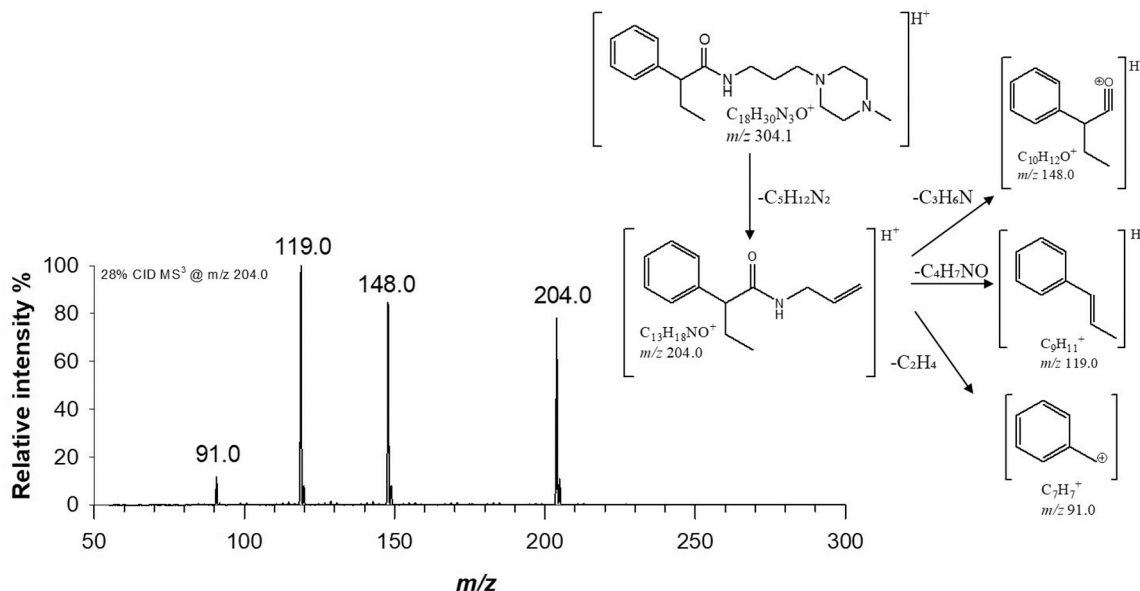


Fig. 2. MS³ spectra of piperazine derivative (1), obtained by fragmenting protonated molecule at m/z 304.0 with a collision energy of 7.4 eV and product ion at m/z 204.0 with a collision energy of 9.8 eV, using a window of ± 6.0 m/z unit centered around each selected value. Inset: proposed structures and fragmentation scheme of product ion at m/z 204.0.

acquisition in the ion trap of the MS³ spectra of the precursor ion at m/z 173.0 with a collision energy of 7.7 eV gave five product ions, namely ion at m/z 117.0 ($C_9H_9^+$), m/z 105.0 ($C_8H_9^+$), m/z 95.0 ($C_7H_{11}^+$), m/z 91.0 ($C_7H_7^+$) and m/z 81.0 ($C_6H_9^+$), whose proposed structures are reported in Figure S1. Precursor ion at m/z 258.0 was isolated and further fragmented with a collision energy of 8.7 eV. The obtained MS³ spectra

showed the presence of a signal at m/z 176.0 ($C_{11}H_{14}NO^+$), which was assigned to fragment obtained by the loss of a C_6H_{10} unit following the cleavage of the bond between the cyclohexyl ring and the carbon skeleton.

For morpholine derivatives (3), (4), (5) and (6), the FT ICR MS spectra were acquired in positive ion mode (ESI⁺) due to their reduced

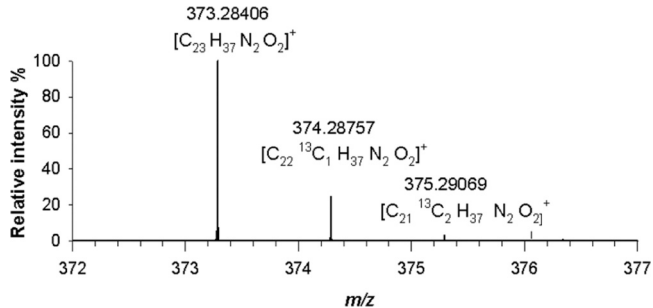
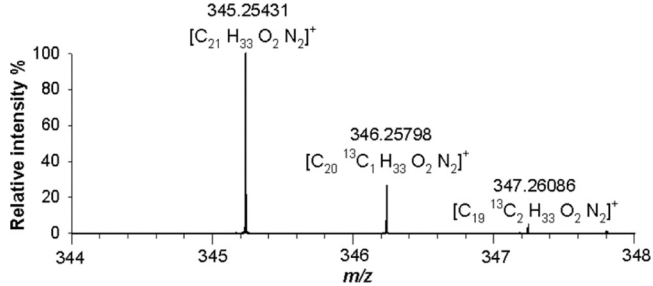
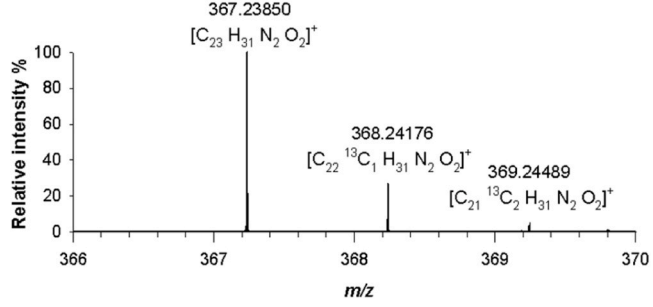
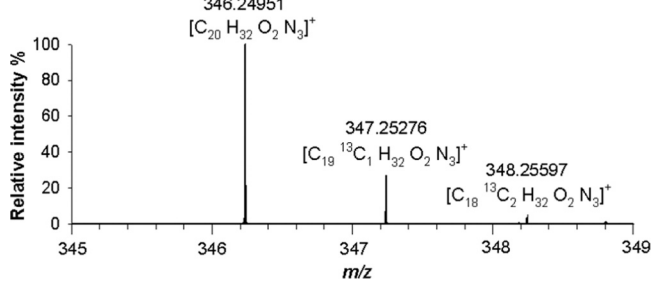
pKa value [17]. For compound (3), a dominant protonated molecule signal at m/z 373.28406 ($[M+H]^+$, $C_{23}H_{31}N_2O_2^+$) with only 2.4 ppm difference from the theoretical value, was observed. The observed isotopic pattern of $[C_{25}H_{37}N_2O_2]^+$ was in good agreement with the predicted one, as the signals at m/z 374.28757 and m/z 375.29069, related to A+1 and A+2 isotopologues, i.e. $[C_{24}^{13}CH_3H_37N_2O_2]^+$ and $[C_{23}^{13}C_2H_37N_2O_2]^+$, had mass errors in RMS not exceeding 2.6 ppm (Table 2). A detailed analysis of isotopologue pattern was needed to confirm the elemental composition of (4), (5) and (6) derivatives, whose protonated molecule signals were observed in the FT ICR MS spectra at m/z 345.25431 ($[M+H]^+$, $C_{21}H_{33}N_2O_2^+$, RMS error 1.9 ppm), m/z

367.23850 ($[M+H]^+$, $C_{23}H_{31}N_2O_2^+$, RMS error 1.4 ppm) and m/z 346.25091 ($[M+H]^+$, $C_{20}H_{32}N_3O_2^+$, RMS error 1.8 ppm), respectively. The agreement between the experimental and theoretical values relating to isotopologues A+1 at m/z 346.25798 ($[C_{20}^{13}CH_3H_32N_3O_2]^+$), m/z 368.24176 ($[C_{22}^{13}CH_3H_31N_2O_2]^+$) and m/z 347.25276 ($[C_{19}^{13}C_2H_32N_3O_2]^+$), and A+2 at m/z 347.26086 ($[C_{19}^{13}C_2H_33N_2O_2]^+$), m/z 369.24489 ($[C_{21}^{13}C_2H_31N_2O_2]^+$) and m/z 348.25597 ($[C_{18}^{13}C_2H_32N_3O_2]^+$), was found with mass errors not exceeding 2.8 ppm (Table 2).

For MSⁿ operation, tandem mass spectra were generated by optimizing collision energies according to the precursor ion (Table S2). For derivatives (3) and (4), MS/MS mass spectra exhibited a single fragment

Table 2

Accurate mass values, relative intensity and mass accuracy, expressed as RMS errors in ppm, of the protonated adducts and isotopologues of new synthesized morpholine ((3), (4), (5) and (6)) derivatives.

Compound Molecular Formula Exact mass	m/z^a	Relative Intensity (%)	Mass accuracy in RMS ^b ppm	ESI-(+)-FT ICR MS spectra
(3) $C_{23}H_{36}N_2O_2$ 372.27768	$[M+H]^+$ 373.28406	100	2.4	
	$[M+H+1]^+$ 374.28757	24.1	2.0	
	$[M+H+2]^+$ 375.29069	3.0	2.6	
(4) $C_{21}H_{32}N_2O_2$ 344.24638	$[M+H]^+$ 345.25431	100	1.9	
	$[M+H+1]^+$ 346.25798	22.2	2.8	
	$[M+H+2]^+$ 347.26086	2.5	1.4	
(5) $C_{23}H_{30}N_2O_2$ 366.23073	$[M+H]^+$ 367.23850	100	1.4	
	$[M+H+1]^+$ 368.24176	24	1.1	
	$[M+H+2]^+$ 369.24489	3	0.5	
(6) $C_{20}H_{31}N_3O_2$ 345.24163	$[M+H]^+$ 346.25091	100	1.8	
	$[M+H+1]^+$ 347.25276	21	1.4	
	$[M+H+2]^+$ 348.25597	2.8	1.0	

^a Calculated as mean of 5 m/z measurements.

^b Mass accuracy reported as root-mean-square (RMS) in parts per million (ppm) of five ($n=5$) m/z measurements.

ion due to the loss of the morpholine unit (-87.0 Da, C_4H_9NO) [18], at m/z 286.1 and m/z 258.0, respectively. By fragmenting precursor ion at m/z 286.1 with a collision energy of 8.8 eV, five major fragments were generated at m/z 204.0 ($C_{13}H_{18}NO^+$), m/z 173.0 ($C_{13}H_{17}^+$), m/z 161.0 ($C_{10}H_{11}NO^+$), m/z 105.0 ($C_8H_9^+$), and m/z 91.0 ($C_7H_7^+$) (Fig. 3). A cyclic rearrangement following the loss of cyclohexyl moiety has been proposed to explain the presence of fragment ion at m/z 204.0. Such a fragment ion was not detected in the MS³ spectra of compound (4), obtained by fragmenting precursor at m/z 258.0. For this derivative, the loss of 153 Da and 85 Da allowed to confirm the N-ethyl substituent (Table S2). The substitution of the cyclohexyl unit with a benzene ring let (5) derivative to fragment according to a different scheme (Table S2), as a base peak at m/z 167.0 ($C_{13}H_{11}^+$) was observed in the MS/MS spectra, corresponding to a stable diphenylmethane cation [19], further fragmented by CID-MS³ experiments. In this case, the loss of the morpholine core gave a signal at m/z 280.0 ($C_{19}H_{22}NO^+$) with a relative intensity of around 5% compared to base peak. Also, for derivative (6), signal at m/z 259.0 ($C_{16}H_{23}N_2O^+$), due to the loss of morpholine, had a relative intensity of 5%, while base peak being signal at m/z 171.0. Such a signal was assigned to fragment ion obtained by amide bond cleavage and was further fragmented with a collision energy of 10.5 eV in order to confirm its identity (Table S2).

Moreover, the diameter of the inhibition zone (expressed in mm) and MIC results are reported in Tables 3–4. Morpholine derivative (3) (Table 3) exhibited a broad spectrum of action, showing a high inhibitory action against 82.83% of the bacterial strains tested, with an inhibition zone between 16 and 31 mm, except for *Micrococcus flavus*, that was inhibited with a medium activity. Particularly, *Enterococcus hirae*, *Enterococcus faecium*, *Enterococcus durans* and *Enterococcus gallinarum* species were inhibited at a low concentration (3.125 mg/ml) after treatment with compound (3); the 44.81% of the bacterial strains was inhibited at a concentration of 6.25 mg/ml; *Escherichia coli*, *Listeria innocua*, *Planococcus psychrotolerans* and *Bacillus amyloliquefaciens* species showed sensitivity to this compound at a concentration of 12.5 mg/ml, while the other strains (*Listeria monocytogenes* and *Micrococcus flavus*) required a higher inhibition concentration.

The morpholine derivatives (4) and (6) (Table 3) showed a middle-high inhibitory action against all tested bacterial strains, except for the *Brochothrix thermosphacta* strain, that proved a low sensitivity to the compound (4).

A high inhibitory activity of derivative (4) was observed against 79.3% of the tested bacterial strains, with an inhibition zone between 17 and 26 mm, while a middle inhibitory activity against *Pseudomonas fragi*, *Hafnia alvei*, *Enterococcus faecalis*, *Listeria innocua* and *Pseudomonas aeruginosa* strains. The 38% of the inhibited strains required a concentration of 12.5 mg/ml, while 34.4% a concentration of 6.25 mg/ml. Only *Enterococcus faecium* and *Enterococcus gallinarum* species were

inhibited at a low concentration of 3.125 mg/ml of this compound (Table 3).

The derivative (6) showed a high inhibitory activity against 89.61% of the bacterial strains tested, while a middle action was observed against *Hafnia alvei*, *Pseudomonas proteamaculans* and *Enterococcus gallinarum*. The 48% of tested strains was sensitive at a concentration of 12.5 mg/ml, whereas three *Enterococcus* species, *Micrococcus flavus*, *Bacillus anthracis* and *Pseudomonas orientalis* showed sensitivity to compound (6) at a concentration of 6.25 mg/ml (Table 3).

The fourth morpholine derivative tested (compound (5)) was active against the 34.40% of the bacterial strains with a high inhibitory activity observed towards the 20.7% of strains (inhibition zone between 21 and 29 mm). The most of sensitive strains required a low concentration of 3.125 mg/ml (Table 3).

Moreover, the antimicrobial activity of two piperazine derivatives was evaluated. The derivative (2) showed a broad action spectrum, with a high inhibitory activity against all bacterial strains tested. In particular, the 44.83% of strains showed sensitivity to this compound at a concentration of 12.5 mg/ml, the 48.27% of strains was inhibited at a concentration of 6.25 mg/ml, while the remaining strains (*Enterococcus casseliflavus* and *Bacillus subtilis*) required a lower inhibition concentration (Table 4).

The other piperazine derivative (1) exhibited an inhibitory activity only against some environment-borne strains; *Bacillus subtilis*, *Bacillus anthracis*, *Pseudomonas orientalis* and *Bacillus cereus* strains demonstrated a low sensitivity to the compound at a concentration of 25 mg/ml, while *Bacillus amyloliquefaciens* strain required a lower inhibition concentration of 12.5 mg/ml (Table 4).

In the search for effective antimicrobial agents, the literature provides information on a number of heterocyclic compounds, including piperazine derivatives, that showed a broad spectrum of pharmacological effects, including antimicrobial activity. Medicinal chemists have had great success in modifying the basic chemical structures of known antibiotics, both natural and synthetic, where the heterocyclic nucleus forms part of the pharmacophore necessary for specific pharmacological activity. Piperazine is a medically important heterocyclic nucleus consisting of a six-membered ring containing two nitrogen atoms in opposite positions in the ring and it's frequently found in biologically active compounds in many different therapeutic areas [20–25].

In this work, results showed that compounds demonstrated antimicrobial activity against many tested bacterial species, providing a different inhibitory effect probably linked to different chemical structure. Some of the tested bacteria are foodborne, the most of them comes from meat/naturally fermented meat products and others from milk/milk products; of these, some strains are food spoilage bacteria and other strains are selected autochthonous starter cultures. The rest of the tested bacterial strains come from an environmental matrix; some are

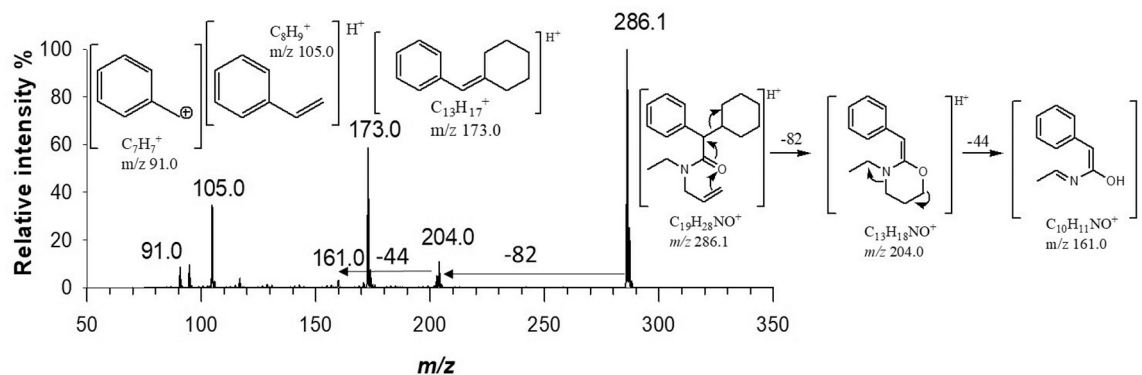


Fig. 3. MS³ spectra of (3) morpholine derivative, obtained by fragmenting protonated molecule at m/z 373.0 with a collision energy of 7.3 eV and product ion at m/z 286.1 with a collision energy of 8.8 eV, using a window of ± 6.0 m/z unit centered around each selected value. Inset: proposed structures and fragmentation scheme of product ion at m/z 286.1.

Table 3
Antimicrobial activity of morpholine derivatives 3–6.

Label	Bacterial strains	Chloramphenicol (positive control) Inhibition Zone ^a	Compound 3		Compound 4		Compound 5		Compound 6	
			Inhibition Zone ^a	MIC (mg/ml)	Inhibition Zone ^a	MIC (mg/ml)	Inhibition Zone ^a	MIC (mg/ml)	Inhibition Zone ^a	MIC (mg/ml)
1	<i>Carnobacterium maltaromaticum</i>	25.83 ± 0.53	20.46 ± 0.98 ^b	6.25 ± 0.08	23.57 ± 0.76	6.25 ± 0.48	27.45 ± 0.76	3.125 ± 0.88	20.23 ± 0.96	12.5 ± 0.55
2	<i>Carnobacterium divergens</i>	29.50 ± 1.61	21.39 ± 0.11	6.25 ± 0.66	19.73 ± 0.98	6.25 ± 0.45	/	/	18.28 ± 0.22	25 ± 0.72
3	<i>Pseudomonas fragi</i>	19.87 ± 1.23	24.70 ± 0.91	6.25 ± 0.78	15.85 ± 0.09	12.5 ± 0.56	/	/	17.77 ± 0.59	25 ± 0.90
4	<i>Hafnia alvei</i>	18.24 ± 1.55	/	/	14.33 ± 0.54	50 ± 0.70	/	/	13.32 ± 0.77	25 ± 0.87
5	<i>Pseudomonas proteamaculans</i>	18.78 ± 1.78	/	/	16.98 ± 0.43	25 ± 0.99	11.28 ± 0.53	50 ± 0.64	14.88 ± 0.23	25 ± 0.46
6	<i>Brochothrix thermosphacta</i>	28.91 ± 1.23	/	/	8.86 ± 0.75	50 ± 0.69	9.66 ± 0.78	50 ± 0.56	17.65 ± 0.59	25 ± 0.78
7	<i>Escherichia coli</i>	18.32 ± 1.03	24.63 ± 0.28	12.5 ± 0.43	21.40 ± 0.38	12.5 ± 0.97	14.98 ± 0.90	25 ± 0.29	17.66 ± 0.80	12.5 ± 0.44
8	<i>Enterococcus hirae</i>	22.45 ± 0.93	20.05 ± 0.09	3.125 ± 0.61	24.46 ± 0.56	6.25 ± 0.76	/	/	24.70 ± 0.82	12.5 ± 0.36
9	<i>Enterococcus faecium</i>	12.47 ± 1.03	20.57 ± 0.08	3.125 ± 0.86	19.06 ± 0.63	3.125 ± 0.46	/	/	27.43 ± 0.66	6.25 ± 0.93
10	<i>Enterococcus faecalis</i>	16.89 ± 1.79	19.79 ± 0.33	6.25 ± 0.98	15.76 ± 0.56	6.25 ± 0.57	/	/	21.78 ± 0.85	6.25 ± 0.76
11	<i>Enterococcus casseliflavus</i>	15.02 ± 0.85	16.44 ± 0.77	6.25 ± 0.33	20.59 ± 0.86	6.25 ± 0.65	8.93 ± 0.33	12.5 ± 0.98	22.84 ± 0.47	6.25 ± 0.99
12	<i>Enterococcus durans</i>	20.98 ± 1.77	17.37 ± 0.45	3.125 ± 0.53	21.66 ± 0.90	25 ± 0.43	/	/	16.72 ± 0.56	25 ± 0.34
13	<i>Enterococcus gallinarum</i>	21.04 ± 1.31	16.91 ± 0.68	3.125 ± 0.42	17.49 ± 0.86	3.125 ± 0.56	/	/	15.38 ± 0.62	12.5 ± 0.62
14	<i>Listeria innocua</i>	25.88 ± 0.93	26.63 ± 0.71	12.5 ± 0.48	13.64 ± 0.33	25 ± 0.57	/	/	17.47 ± 0.53	25 ± 0.87
15	<i>Staphylococcus aureus</i>	22.04 ± 0.66	22.76 ± 0.90	6.25 ± 0.90	17.33 ± 0.63	12.5 ± 0.88	/	/	16.23 ± 0.56	12.5 ± 0.68
16	<i>Escherichia coli</i>	19.03 ± 0.56	25.30 ± 0.88	6.25 ± 0.79	17.82 ± 0.86	12.5 ± 0.89	/	/	22.56 ± 0.58	12.5 ± 0.97
17	<i>Listeria monocytogenes</i>	21.41 ± 1.02	20.29 ± 0.43	25 ± 0.20	23.71 ± 0.56	12.5 ± 0.74	/	/	20.09 ± 0.90	25 ± 0.47
18	<i>Salmonella serovar</i>	20.39 ± 0.36	19.77 ± 0.93	6.25 ± 0.99	16.99 ± 0.56	25 ± 0.32	/	/	18.78 ± 0.57	50 ± 0.85
19	<i>Pseudomonas aeruginosa</i>	22.33 ± 0.98	/	/	15.55 ± 0.59	6.25 ± 0.71	/	/	20.44 ± 0.83	12.5 ± 0.50
20	<i>Micrococcus flavus</i>	20.65 ± 0.47	15.78 ± 0.22	25 ± 0.68	20.34 ± 0.28	12.5 ± 0.86	/	/	20.60 ± 0.77	6.25 ± 0.88
21	<i>Lysinibacillus fusiformis</i>	23.02 ± 0.92	/	/	23.82 ± 0.94	12.5 ± 0.63	/	/	24.83 ± 0.89	25 ± 0.68
22	<i>Bacillus subtilis</i>	24.43 ± 0.38	28.81 ± 0.40	3.125 ± 0.49	26.90 ± 0.75	6.25 ± 0.90	28.04 ± 0.69	3.125 ± 0.96	20.32 ± 0.62	12.5 ± 0.33
23	<i>Planococcus psychrotoleratus</i>	23.71 ± 0.90	24.82 ± 0.87	12.5 ± 0.92	20.24 ± 0.38	12.5 ± 0.56	/	/	21.78 ± 0.44	12.5 ± 0.87
24	<i>Bacillus amyloliquefaciens</i>	24.32 ± 0.63	23.74 ± 0.24	12.5 ± 0.75	25.62 ± 0.84	6.25 ± 0.55	28.35 ± 0.66	3.125 ± 0.22	27.08 ± 0.70	12.5 ± 0.58
25	<i>Bacillus anthracis</i>	24.04 ± 0.69	29.82 ± 0.12	6.25 ± 0.47	22.74 ± 0.90	6.25 ± 0.61	21.52 ± 0.89	3.125 ± 0.76	24.55 ± 0.43	6.25 ± 0.46
26	<i>Bacillus amyloliquefaciens</i>	24.87 ± 0.95	31.35 ± 0.44	6.25 ± 0.21	25.26 ± 0.75	12.5 ± 0.42	25.98 ± 0.45	3.125 ± 0.85	25.79 ± 0.75	12.5 ± 0.99
27	<i>Pseudomonas orientalis</i>	25.03 ± 0.21	29.78 ± 0.92	6.25 ± 0.98	26.93 ± 0.53	6.25 ± 0.68	29.57 ± 0.80	3.125 ± 0.43	24.33 ± 0.94	6.25 ± 0.85
28	<i>Bacillus cereus</i>	22.98 ± 0.98	23.56 ± 0.82	6.25 ± 0.77	23.72 ± 0.78	12.5 ± 0.99	/	/	23.84 ± 0.65	12.5 ± 0.43
29	<i>Bacillus cereus</i>	23.03 ± 0.73	25.71 ± 0.90	6.25 ± 0.57	25.07 ± 0.39	12.5 ± 0.50	/	/	30.37 ± 0.96	12.5 ± 0.79

/: no inhibition zone was observed

^a diameter in mm

^b Values are presented as mean ± standard deviation

destructive, while others are beneficial and responsible of different processes.

The results observed in this study underline the importance and the fundamental role of the derivatives structure in their biological activity. As already known in the literature, compounds containing the morpholine ring have a wide spectrum of biological activity, including the inhibition of microbial protein synthesis [26]. The compound (4) has the morpholine ring, an aromatic ring and a 6-member ring, a

three-membered alkyl chain (n=3) and a retro-amide (NH₂CO) which enhance biological activity [15,27]. Compound (5) showed a minor but selective antimicrobial activity, despite having a five-membered alkyl chain (n=5), as the literature reports that a greater length of the alkyl chain corresponds to greater antibacterial activity. Birnie et al. [28] reported that the presence of long alkyl chains promotes the biological activity of derivatives by increasing lipophilicity and the ability of the compounds to destroy the cell wall of microorganisms. Compounds (4)

Table 4
Antimicrobial activity of piperazine derivatives 1 and 2.

Label	Bacterial strains	Chloramphenicol (positive control) Inhibition Zone ^a	Compound 1		Compound 2	
			Inhibition Zone ^a	MIC (mg/ml)	Inhibition Zone ^a	MIC (mg/ml)
1	<i>Carnobacterium maltaromaticum</i>	25.83 ± 0.53	/	/	25.42 ± 0.77	6.25 ± 0.60
2	<i>Carnobacterium divergens</i>	29.50 ± 1.61	/	/	20.94 ± 0.34	6.25 ± 0.84
3	<i>Pseudomonas fragi</i>	19.87 ± 1.23	/	/	22.73 ± 0.84	6.25 ± 0.53
4	<i>Hafnia alvei</i>	18.24 ± 1.55	/	/	19.68 ± 0.66	12.5 ± 0.99
5	<i>Pseudomonas proteamaculans</i>	18.78 ± 1.78	/	/	19.88 ± 0.53	12.5 ± 0.64
6	<i>Brochothrix thermosphacta</i>	28.91 ± 1.23	/	/	19.91 ± 0.78	12.5 ± 0.56
7	<i>Escherichia coli</i>	18.32 ± 1.03	/	/	22.57 ± 0.90	6.25 ± 0.29
8	<i>Enterococcus hirae</i>	22.45 ± 0.93	/	/	20.67 ± 0.77	12.5 ± 0.85
9	<i>Enterococcus faecium</i>	12.47 ± 1.03	/	/	20.32 ± 0.90	12.5 ± 0.72
10	<i>Enterococcus faecalis</i>	16.89 ± 1.79	/	/	21.18 ± 0.56	12.5 ± 0.89
11	<i>Enterococcus casseliflavus</i>	15.02 ± 0.85	/	/	24.46 ± 0.33	3.125 ± 0.98
12	<i>Enterococcus durans</i>	20.98 ± 1.77	/	/	21.30 ± 0.90	12.5 ± 0.29
13	<i>Enterococcus gallinarum</i>	21.04 ± 1.31	/	/	18.77 ± 0.55	12.5 ± 0.80
14	<i>Listeria innocua</i>	25.88 ± 0.93	/	/	22.64 ± 0.76	12.5 ± 0.68
15	<i>Staphylococcus aureus</i>	22.04 ± 0.66	/	/	18.97 ± 0.77	12.5 ± 0.34
16	<i>Escherichia coli</i>	19.03 ± 0.56	/	/	21.44 ± 0.46	12.5 ± 0.88
17	<i>Listeria monocytogenes</i>	21.41 ± 1.02	/	/	20.12 ± 0.95	12.5 ± 0.58
18	<i>Salmonella serovar</i>	20.39 ± 0.36	/	/	22.78 ± 0.35	6.25 ± 0.72
19	<i>Pseudomonas aeruginosa</i>	22.33 ± 0.98	/	/	19.89 ± 0.59	12.5 ± 0.82
20	<i>Micrococcus flavus</i>	20.65 ± 0.47	/	/	25.22 ± 0.66	6.25 ± 0.77
21	<i>Lysinibacillus fusiformis</i>	23.02 ± 0.92	/	/	26.41 ± 0.55	6.25 ± 0.32
22	<i>Bacillus subtilis</i>	24.43 ± 0.38	9.40 ± 0.67 ^b	25 ± 0.84	35.24 ± 0.69	3.125 ± 0.96
23	<i>Planococcus psychrotoleratus</i>	23.71 ± 0.90	/	/	32.31 ± 0.55	6.25 ± 0.43
24	<i>Bacillus amyloliquefaciens</i>	24.32 ± 0.63	/	/	34.30 ± 0.66	6.25 ± 0.78
25	<i>Bacillus anthracis</i>	24.04 ± 0.69	17.27 ± 0.89	25 ± 0.79	30.27 ± 0.89	6.25 ± 0.94
26	<i>Bacillus amyloliquefaciens</i>	24.87 ± 0.95	10.78 ± 0.45	12.5 ± 0.82	34.46 ± 0.45	6.25 ± 0.65
27	<i>Pseudomonas orientalis</i>	25.03 ± 0.21	9.95 ± 0.80	25 ± 0.43	25.59 ± 0.80	6.25 ± 0.88
28	<i>Bacillus cereus</i>	22.98 ± 0.98	9.73 ± 0.66	25 ± 0.72	24.67 ± 0.51	6.25 ± 0.62
29	<i>Bacillus cereus</i>	23.03 ± 0.73	9.88 ± 0.90	25 ± 0.27	23.79 ± 0.35	6.25 ± 0.70

/: no inhibition zone was observed

^a diameter in mm

^b Values are presented as mean ± standard deviation

and (6), with antibacterial activity against all bacterial strains tested, have a three-membered alkyl chain (n=3); the antibacterial action of the compound (4) is enhanced by the presence of the amide group (CONH₂) [29], while the activity of the compound (6) is enhanced by the presence of urea [22,32]. Some studies have shown that the heterocyclic ring is the target of many reactions, leading to the obtaining of biologically active compounds with antimicrobial effects due to the modifications of chemical structure [30,31].

For structural characterization of piperazine and morpholine derivatives, High-Resolution Mass Spectrometry with electrospray ionization in positive ion mode (ESI⁺) using a Fourier Transform Cyclotron Ion Resonance (FT ICR) analyzer has been employed. FT-ICR MS is capable of achieving low ppm mass accuracy and high re-solving power as the detection signal in the analyzer cell typically lasts for several seconds, resulting in numerous cycles of cyclotron motion. Therefore, a significant limitation in the number of empirical formulas that can be associated with a *m/z* could be reached [32]. As with FT-ICR MS just MS/MS experiments can be conducted, in this work a comprehensive structural characterization of all newly synthesized drugs has been supported by MSⁿ analysis performed with a positive-mode electrospray ionization mass spectrometer with a quadrupole linear ion trap analyzer (ESI-(+)-LTQ-MS/MS).

Mass spectrometric techniques play a crucial role in the structural characterization of newly synthesized compounds, as they allow to confirm the success of the synthesis by accurate mass measurements, isotopic distribution evaluation, and tandem mass spectrometric data (MSⁿ), and together with hyphenated techniques, to evaluate the metabolomic pathway [33,34]. The overall structure of the potential drugs, including atoms arrangements, can be elucidated by MSⁿ experiments. High-Resolution Mass Spectrometry (HRMS) is a well-established and widely accepted analytical technique for novel

drugs characterization, due to higher resolving power and higher mass accuracy, and to the possibility to isolate and observe ions for extended periods [35]. Using HRMS can help meet regulatory requirements, ensuring compound's safety and efficacy, thus significantly enhances drug development process and helping bring safer and more effective pharmaceuticals to the market.

In conclusion, six new derivatives with a piperazine and morpholine core unit, respectively, have been synthesized in this work. ESI-LTQ-MS in combination with ESI-FT-ICR-MS was proved to play a significant role in the structural characterization of novel piperazine and morpholine derivatives and for the study of fragmentation pathways. Accurate mass measurements, isotope distributions and characteristic fragment ions obtained by MSⁿ experiments were consistent with the basic molecular structure. Results of antimicrobial activity assay showed that the different chemical structure of derivatives seems to play an important role in the width of the action spectrum of each compound on bacterial strains, revealing that the new-synthesized derivatives could be promising candidates to be used as antimicrobial agents.

Funding

This research did not receive any specific grant from funding agencies in the public, commercial, or not-for-profit sectors.

CRediT authorship contribution statement

Giovanni Salzano: Supervision, Formal analysis, Data curation. **Giuliana Bianco:** Writing – review & editing, Visualization, Supervision, Methodology. **Patrizia Iannece:** Formal analysis, Data curation. **Carmine Gaeta:** Formal analysis, Data curation. **Federica Giuzio:** Investigation, Data curation. **Angela Di Capua:** Investigation, Formal

analysis, Data curation. **Carmela Saturnino**: Writing – review & editing, Visualization. **Maria Assunta Acquavia**: Writing – original draft, Investigation, Data curation. **Maria Grazia Bonomo**: Writing – review & editing, Supervision, Methodology.

Declaration of Competing Interest

The authors declare that they have no known competing financial interests or personal relationships that could have appeared to influence the work reported in this paper.

Acknowledgments

The authors would like to thank Graziana Cardone and Barbara Emanuela Scalese for their support in mass spectrometric data elaboration and antimicrobial activity assay

Appendix A. Supporting information

Supplementary data associated with this article can be found in the online version at [doi:10.1016/j.jpba.2024.116202](https://doi.org/10.1016/j.jpba.2024.116202).

References

- [1] J. Davies, Where have all the raises gone? *Can. J. Infect. Dis. Med. Microbiol.* 17 (2006) 287–290, <https://doi.org/10.1155/2006/707296>.
- [2] M. Hutchings, A. Truman, B. Wilkinson, Antibiotics: past, present and future, *Curr. Opin. Microbiol.* 51 (2019) 72–80, <https://doi.org/10.1016/j.mib.2019.10.008>.
- [3] H.R. Gaskins, C.T. Collier, D.B. Anderson, Antibiotics as growth promotants: mode of action, *Anim. Biotechnol.* 13 (2002) 29–42, <https://doi.org/10.1081/ABIO-120005768>.
- [4] J.F. Prescott, The resistance tsunami, antimicrobial stewardship, and the golden age of microbiology, *Vet. Microbiol.* 171 (2014) 273–278, <https://doi.org/10.1016/j.vetmic.2014.02.035>.
- [5] A. Macgowan, Antibiotic resistance, *Medicine* 45 (2017) 622–628, <https://doi.org/10.1016/j.mpmed.2017.07.006>.
- [6] S.B. Singh, K. Young, L.L. Silver, What is an “ideal” antibiotic? Discovery challenges and path forward, *Biochem. Pharmacol.* 133 (2017) 63–73, <https://doi.org/10.1016/j.bcp.2017.01.003>.
- [7] K.E. Gettys, Z. Ye, M. Dai, Recent advances in piperazine synthesis, *Synthesis* 49 (2017) 2589–2604, <https://doi.org/10.1055/s-0036-1589491>.
- [8] U.I.S. Al-Neaimy, Z.F. Saeed, S.M. Shehab, A review on analytical methods for piperazine determination, *NTU J. Pure Sci.* 1 (2022) 1–9, <https://doi.org/10.56286/ntujps.v1i3.230>.
- [9] M.A. Walker, Novel tactics for designing water-soluble molecules in drug discovery, *Expert Opin. Drug Discov.* 9 (2014) 1421–1433, <https://doi.org/10.1517/17460441.2014.960839>.
- [10] A.P. Kourounakis, D. Xanthopoulos, A. Tzara, Morpholine as a privileged structure: a review on the medicinal chemistry and pharmacological activity of morpholine containing bioactive molecules, *Med. Res. Rev.* 40 (2020) 709–752, <https://doi.org/10.1002/med.21634>.
- [11] M. Al-Ghorbani, B. Begum Zabiulla, V.S. Mamatha, S.A. Khanum, Piperazine and morpholine: synthetic preview and pharmaceutical applications, *J. Chem. Pharm. Res.* 7 (2015) 281–301, <https://doi.org/10.5958/0974-360X.2015.00100.6>.
- [12] R. Kumar, R. Srinivasa, K.S. Vulichi, Emphasizing morpholine and its derivatives (MAID): a typical candidate of pharmaceutical importance, *Int. J. Chem. Sci.* 14 (2016) 1777–1788.
- [13] C. Saturnino, A. Capasso, J.C. Lancelot, S. Rault, M. Buonerba, G. De Martino, Pharmacological studies and synthesis of morpholino alkyl derivatives, *Chem. Pharm. Bull.* 50 (2002) 1151–1154, <https://doi.org/10.1248/cpb.50.1151>.
- [14] M.G. Bonomo, C. Cafaro, D. Russo, L. Calabrone, L. Milella, C. Saturnino, A. Capasso, G. Salzano, Antimicrobial activity, antioxidant properties and phytochemical screening of *Aesculus hippocastanum* mother tincture against food-borne bacteria, *Lett. Drug Des. Discov.* 17 (2018) 48–56, <https://doi.org/10.2174/157018081666618110814115>.
- [15] M.G. Bonomo, T. Giura, G. Salzano, P. Longo, A. Mariconda, A. Catalano, D. Iacopetta, J. Ceramella, M.S. Sinicropi, C. Saturnino, Bis-Thiourea Quaternary ammonium salts as potential agents against bacterial strains from food and environmental matrices, *Antibiotics* 10 (2021) 1466, <https://doi.org/10.3390/antibiotics10121466>.
- [16] A. Welz, M. Koba, P. Košlirski, J. Siódmiak, Rapid targeted method of detecting abused piperazine designer drugs, *J. Clin. Med.* 10 (2021), <https://doi.org/10.3390/jcm10245813>.
- [17] B. König, G. Sztanó, T. Holczbauer, T. Soós, Syntheses of 2- and 3-substituted morpholine congeners via ring opening of 2-Tosyl-1,2-oxazetidine, *J. Org. Chem.* 88 (2023) 6182–6191, <https://doi.org/10.1021/acs.joc.3c00207>.
- [18] W.M.A. Niessen, H. Rosing, J.H. Beijnen, Interpretation of MS–MS spectra of small-molecule signal transduction inhibitors using accurate-m/z data and m/z-shifts with stable-isotope-labeled analogues and metabolites, *Int. J. Mass Spectrom.* 464.2021, 116559 [10.1016/j.ijms.2021.116559](https://doi.org/10.1016/j.ijms.2021.116559).
- [19] E.H. Kim, H.S. Seo, N.Y. Ki, N.H. Park, W. Lee, J.A. Do, S. Park, S.Y. Baek, B. Moon, H. Oh, et al., Reliable screening and confirmation of 156 multi-class illegal adulterants in dietary supplements based on extracted common ion chromatograms by ultra-high-performance liquid chromatography-quadrupole/time of flight-mass spectrometry, *J. Chromatogr. A* 1491 (2017) 43–56, <https://doi.org/10.1016/j.chroma.2017.02.032>.
- [20] A. Paneth, N. Trotsko, Ł. Popiołek, A. Grzegorzczak, T. Krzanowski, S. Janowska, A. Malm, M. Wujec, Synthesis and antibacterial evaluation of Mannich bases derived from 1,2,4-Triazole, *Chem. Biodivers.* 16 (2019), <https://doi.org/10.1002/cbdv.201900377>.
- [21] M. Patil, A. Noonikara-Poyil, S.D. Joshi, S.A. Patil, S.A. Patil, A. Bugarin, New urea derivatives as potential antimicrobial agents: synthesis, biological evaluation, and molecular docking studies, *Antibiotics* 8 (2019), <https://doi.org/10.3390/antibiotics8040178>.
- [22] U. Kosikowska, M. Wujec, N. Trotsko, W. Płonka, P. Paneth, A. Paneth, Antibacterial activity of fluorobenzoylthiosemicarbazides and their cyclic analogues with 1,2,4-triazole scaffold, *Molecules* 26 (2021) 1–18, <https://doi.org/10.3390/molecules26010170>.
- [23] M. Wujec, U. Kosikowska, A. Siwek, A. Malm, New derivatives of Thiosemicarbazide and 1,2,4-Triazoline-5-thione with potential antimicrobial activity, *Phosphorus Sulfur Silicon Relat. Elem.* 184 (2009) 559–567, <https://doi.org/10.1080/10426500802208490>.
- [24] R. Kharb, K. Bansal, A.K. Sharma, A valuable insight into recent advances on antimicrobial activity of piperazine derivatives, *Der Pharma Chem.* 4 (2012) 2470–2488.
- [25] A. Lukin, M. Chudinov, T. Vedekhina, E. Rogacheva, L. Kraeva, O. Bakulina, M. Krasavin, Exploration of spirocyclic derivatives of ciprofloxacin as antibacterial agents, *Molecules* 27 (2022) 1–20, <https://doi.org/10.3390/molecules27154864>.
- [26] S.M.R. Hashemian, T. Farhadi, M. Ganjparvar, Linezolid: a review of its properties, function, and use in critical care, *Drug Des. Dev. Ther.* 12 (2018) 1759–1767.
- [27] S.K. Lee, K.H. Choi, S.J. Lee, S.W. Suh, B.M. Kim, B.J. Lee, Peptide deformylase inhibitors with retro-amide scaffold: synthesis and structure-activity relationships, *Bioorg. Med. Chem. Lett.* 20 (2010) 4317–4319, <https://doi.org/10.2147/DDDT.S164515>.
- [28] C.R. Birnie, D. Malamud, R.L. Schnaer, Antimicrobial evaluation of N-Alkyl betaines and N-Alkyl-N,N-dimethylamine oxides with variations in chain length, *Antimicrob. Agents Chemother.* 44 (2000) 2514–2517, <https://doi.org/10.1128/aac.44.9.2514-2517.2000>.
- [29] Y.J. Cui, X.P. Rao, S. Shang, Z.Q. Bin, M.G. Song, H. Shen, Liu, Synthesis, structure analysis and antibacterial activity of N-[5-dehydroabietyl-1,3,4]thiadiazol-2-yl]-aromatic amide derivatives, *J. Saudi Chem. Soc.* 21 (2017) S258–S263, <https://doi.org/10.1016/j.jscs.2014.02.012>.
- [30] H. Bayrak, A. Demirbas, S.A. Karaoglu, N. Demirbas, Synthesis of some new 1,2,4-triazoles, their Mannich and Schiff bases and evaluation of their antimicrobial activities, *Eur. J. Med. Chem.* 44 (2009) 1057–1066, <https://doi.org/10.1016/j.ejmech.2008.06.019>.
- [31] C. Saturnino, F. Grande, S. Aquaro, A. Caruso, D. Iacopetta, M.G. Bonomo, P. Longo, D. Schols, M.S. Sinicropi, Chloro-1,4-dimethyl-9H-carbazole derivatives displaying anti-HIV activity, *Molecules* 23 (2018), <https://doi.org/10.3390/molecules23020286>.
- [32] A. Onzo, M.A. Acquavia, R. Pascale, P. Iannece, C. Gaeta, K.O. Nagornov, Y. O. Tsybin, G. Bianco, Metabolic profiling of Peperoni di Senise PGI bell peppers with ultra-high resolution absorption mode Fourier transform ion cyclotron resonance mass spectrometry, *Int. J. Mass Spectrom.* 470 (2021) 116722, <https://doi.org/10.1016/j.ijms.2021.116722>.
- [33] X. Sun, L. Niu, X. Li, X. Lu, F. Li, Characterization of metabolic profile of mosapride citrate in rat and identification of two new metabolites: Mosapride N-oxide and morpholine ring-opened mosapride by UPLC-ESI-MS/MS, *J. Pharm. Biomed. Anal.* 50 (1) (2009) 27–34, <https://doi.org/10.1016/j.jpba.2009.03.011>.
- [34] I.E. Moreno, B.M. da Fonseca, M. Barroso, S. Costa, J.A. Queiroz, E. Gallardo, Determination of piperazine-type stimulants in human urine by means of microextraction in packed sorbent and high-performance liquid chromatography-diode array detection, *J. Pharm. Biomed. Anal.* 61 (5) (2012) 93–99, <https://doi.org/10.1016/j.jpba.2011.12.004>.
- [35] Z. Lin, C. Zhu, H. Xia, HRMS studies on the fragmentation pathways of metallapentalene, *Spectrochim. Acta Part A Mol. Biomol. Spectrosc.* 136 (2015) 906–910, <https://doi.org/10.1016/j.saa.2014.09.112>.